

Boson expansion description of collective states in osmium and platinum isotopes

K. J. Weeks and T. Tamura

Department of Physics, University of Texas, Austin, Texas 78712

(Received 7 February 1980)

The boson expansion theory, based on which successful explanations were made earlier of collective properties of Ru, Pd, Sm, and other isotopes, is applied here to the Os and Pt isotopes. The nuclei are characterized by the fact that their energy spectra and the $E2$ transitions embody in themselves a very strong γ -unstable nature, nevertheless having quadrupole moments $Q(2_1^+)$ which are large, being negative in Os and positive in the Pt isotopes. It is shown that all these properties can be predicted using the present approach.

[NUCLEAR STRUCTURE $^{186-194}\text{Os}$, $^{188-198}\text{Pt}$, energy levels, $B(E)$'s, branching ratios, magnetic moments, static quadrupole moments, boson expansion theory.]

I. INTRODUCTION

The Os-Pt region appears to be a fascinating region of the periodic table, as regards low energy collective properties in even-even nuclei. The boson expansion theory (BET) was formulated¹⁻³ for practical use and applied²⁻⁴ to a wide class of nuclei, ranging from those that are mildly deformed to those that are well deformed. Nuclei considered in detail in these works^{3,4}; Sm, Ru, and Pd isotopes, however, all had a definite sign of deformation, i.e., prolateness. The Os-Pt nuclei, though similar in many aspects to these nuclei, are interesting in that there is a large scale competition between prolate and oblate shapes; this produces a definite change in sign of the quadrupole moment $Q(2_1^+)$, for the first excited 2^+ state, in going from Os to Pt.

Another feature which makes this region very interesting is that the nuclei there appear to have a strong γ -unstable nature.⁵ In the limit of pure γ instability, however, the prolate and oblate components are perfectly in balance with each other, as well as with the axially nonsymmetric components, resulting in a vanishing $Q(2_1^+)$. Nevertheless, experiment shows that most of the (stable) nuclei in the Os-Pt region have rather large $|Q(2_1^+)|$. These two points are apparently contradictory, and theory should explain these features on a single footing. It is one of the major purposes of the present paper to show that BET satisfies this requirement to a large extent.

Previous theoretical work in this region, for the low-lying positive parity levels of even-even nuclei, has been performed utilizing various approaches. These include the numerical solution of the Bohr Hamiltonian in the framework of the Kumar-Baranger theory, variations of the asymmetric rotor model, and the O(6) to rotor transi-

tion within the interacting boson approximation (IBA). These methods have been applied with various success and have added to our understanding of this complex region. They will be discussed in Sec. IV.

We shall summarize some of the significant experimental features, including those discussed above, that have been seen in the Os-Pt nuclei. Some of these features were already emphasized by Casten *et al.*^{6,7}: (i) The spectra of yrast bands are closer to those of deformed rather than of spherical nuclei. (ii) A well developed γ band appears in every nucleus, except possibly for ^{198}Pt . (iii) The γ band-head energy decreases as the mass number is increased until ^{194}Os is reached where it rises abruptly. In Pt this energy is relatively constant till ^{196}Pt , where it begins to rise. (iv) In general the energy of the first excited 0^+ (0_2^+) state is rather high. (v) $Q(2_1^+)$ is negative in Os and is positive in Pt (as far as the data are available). (vi) Sets of $0^+-2^+-2^+$ triad states appear, particularly in ^{190}Os and ^{196}Pt . (vii) The second excited 0^+ (0_3^+) state decays predominantly to the 2_2^+ (i.e., the 2_7^+) state in $^{188,190}\text{Os}$, while it goes to the 2_1^+ state in $^{194,196}\text{Pt}$. (viii) The so-called $K=4$ band appears in the Os isotopes. (ix) The mode of decay of the 4_2^+ state varies in an interesting fashion as a function of mass number. (x) An irregular sign change takes place for the so-called Coulomb interference term in the Pt isotopes.

It will be appropriate to remark here the way in which we denote individual states. In most of the cases we use the notation I_n^+ to mean the n th state among those with spin (and parity) I^+ ; thus 0_1^+ means the ground state. When a state is known to belong to the γ band, however, we may also denote it as I_γ^+ , whenever it will make our arguments more transparent. It will also be seen that specific notation is used to denote states in the $0^+-2^+-2^+$ triads,

mentioned in the above item (iv), again with the purpose of making the presentation clear.

In Sec. II some details of the present calculation are presented. Results of the calculations are then presented in Sec. III, comparing them with experiment. In Sec. IV comparison is made of our results with those of other related theories. Concluding discussions are made in Sec. V.

II. SOME DETAILS OF THE CALCULATIONS

Since the formulation, based on which the calculations to be presented below were performed, has been explained in detail earlier,¹⁻³ we shall not repeat it here. We shall nevertheless, explain the philosophy behind our approach.

We have in mind the Bohr-Mottelson model⁸ as a guide. Shortly after this phenomenological model was proposed, the Nilsson model⁹ which is a single-particle shell model in a deformed potential was introduced. An extremely important step was then made by Mottelson and Nilsson,¹⁰ who showed that by filling the lowest possible Nilsson orbits it was possible to explain in a very natural way the onset of deformation at the neutron number $N=90$. The significance of this work is that it showed clearly that it is vital to start with realistic single-particle energies if one attempts to predict what sort of collectivity (or deformability) a nucleus with a given pair of N and Z should have. This is one of the minimum requirements that a microscopic theory must satisfy. Our BET of course satisfies this.

The Mottelson-Nilsson work, which does not include the effect of residual interactions, is not by itself sufficient to describe the details of the various collective nuclei. Many attempts thus followed it in order to take such residual interactions into account. We do not intend to go into the history of such attempts. We just want to remark that a theory starting from realistic single-particle energies and then using appropriate (effective) interactions can be denoted as a microscopic theory, and that our BET is such a theory.

Starting in the way described above, and using the BCS theory, our Hamiltonian is written in a form quadratic in quasiparticle fermion pair operators. The next step which the BET takes is to expand the fermion pair operators in a certain (power) series of boson operators, hence the name of BET. The algebra which follows has been explained earlier. Here we want to emphasize that the word "expansion" contains in it an important physical significance.

The motivation of introducing bosons, thus replacing the original fermion Hamiltonian by a new boson Hamiltonian, is to facilitate the ensuing

numerical calculations. However, a nucleus consists of fermions and not bosons. Therefore the new boson Hamiltonian must retain the fermion nature of the original system. This is guaranteed if the above expansion is made in such a way that the boson expanded form of the fermion operators, satisfies the commutation relations which the fermion pairs themselves satisfy. (This was indeed made in Ref. 1). Obviously, a single boson operator which obeys the boson statistics can never satisfy by itself the above requirement. It can do so, nevertheless, if it is combined with multiboson terms. This is why "expansion" is needed.¹¹

The need of the expansion thus originates from the fact that we want to describe a system obeying fermion statistics by quantities that obey boson statistics. Therefore, the appearance of the expansion is more natural than not. If we can accept an infinite expansion, this mapping of the fermion system onto the boson system is exact. In practice we would like to have a finite Hermitian expansion. In Refs. 3 and 4, it was confirmed numerically, by comparing the results of the fourth and sixth order calculations, that the expansion could in fact be terminated at a lower order, and a more formal argument for this has been made in Ref. 11. The critical point of the argument is that only collective fermion-pair operators should be expanded and only a subset of all possible boson excitations be used in the expansion.

The above summarizes the basic concepts of BET, already given in our earlier publications.^{1-4,11} We shall now proceed to the discussion of the input made in applying the BET to the Os-Pt nuclei.

As for the single-particle energies, we took them from a study of experimental¹² single-particle states in the neighborhood of the doubly closed shell ²⁰⁸Pb. These energies are summarized in Table I. To be noted there is the fact that we gave the $i_{13/2}$ neutron energy a linear dependence on A in such a way that it equals -1.62 MeV for $A=208$. We did this because we found that a good choice of the $i_{13/2}$ energy (relative to the others) was rather important in improving the quality of the resultant spectra. The A dependence we chose is consistent with what Veje¹² found when calculating the single-particle energies in a spherically symmetric Woods-Saxon potential. It was shown that the $i_{13/2}$ energy increases rather fast as A is decreased, because the change of the potential radius has a greater effect on the orbits with the largest angular momentum.

The single-particle wave functions were taken to be those of spherical oscillator states. Following the work of Baranger and Kumar,¹³ we took into account the difference in oscillator parameter

TABLE I. Single-particle levels labeled by (Nlj) and their energies in units of $\hbar\omega = 41/A^{1/3}$ MeV. $a = 0.0034(208 - A)$.

Protons				Neutrons			
$4g_{9/2}$	-1.024	$5h_{9/2}$	0.614	$5h_{11/2}$	-1.317	$6i_{13/2}$	-0.234 + a
$4g_{7/2}$	-0.439	$5f_{7/2}$	0.732	$5h_{9/2}$	-0.541	$6g_{9/2}$	0.532
$4d_{5/2}$	-0.219	$5f_{5/2}$	1.024	$5f_{7/2}$	-0.322	$6i_{11/2}$	0.644
$5h_{11/2}$	-0.195			$5p_{3/2}$	-0.124	$6d_{5/2}$	0.810
$4d_{3/2}$	-0.068			$5f_{5/2}$	-0.102	$6g_{7/2}$	0.946
$4s_{1/2}$	0.0			$5p_{1/2}$	0.0	$6d_{3/2}$	0.995

needed to ensure that neutron and proton radii were the same. Also we multiplied matrix elements $\langle k || r^2 || i \rangle$ by the factor $c/(N_p + N_n + 3)$, where $c = 11$ for protons and $c = 13$ for neutrons. In this way the average radius of the different particles and holes has the correct value.^{13,14}

As done before, we fixed the energy gap from the experimental separation energies,¹² instead of introducing explicitly the strength of the monopole pairing interaction. The strengths of the particle-hole and pairing type quadrupole interactions were written as $\chi_2^{pp} = \chi_2^{nn} = \chi_2 = f_2 \chi_2^{sc}$ and $G_2^{pp} = G_2^{nn} = G_2 = g_2 \chi_2^{sc}$, where $\chi_2^{sc} = 240/A^{5/3}$ MeV. The parameter f_2 is expected to be close to unity, while analyses of two-nucleon transfer reactions gave $g_2 = 0.8$, although it can be reduced by as much as a factor of 2 when the number of single-particle orbits taken into account in the calculation is increased.¹⁵ We let f_2 and g_2 be parameters that can take values in the vicinity of the above estimates. Previously we took $f_2 = 0.84 \pm 0.07$, $g_2 = 0.80 \pm 0.07$ for ¹⁰²⁻¹¹⁰Pd and ⁹⁸⁻¹⁰⁴Ru, and $f_2 = 0.91 \pm 0.07$, $g_2 = 1.00 \pm 0.04$ for ¹⁴⁸⁻¹⁵⁴Sm. The values used in this work were the following: $f_2 = 0.91, 0.91, 1.00, 1.02, 0.91, 0.90, 0.98, 1.02, 1.03, 0.99, 1.00$ and $g_2 = 0.54, 0.60, 0.57, 0.59, 0.64, 0.73, 0.68, 0.76, 0.77, 0.77, 0.87$ for ¹⁸⁶⁻¹⁹⁴Os and ¹⁸⁸⁻¹⁹⁸Pt, respectively. The variation of the values of these parameters to the extent shown above is considered rather small when one notes the fact that we fit properties of the various collective nuclei with A ranging from 100 to 200. We were able to do this because we started with realistic single-particle energies, as we emphasized in the beginning of this section.

Electromagnetic transitions are calculated using the microscopically derived $E2$ operators for protons (Q_{pro}) and neutrons (Q_{neu}). It is given as

$$Q_2 = Q_{pro} + e_{eff}(Q_{pro} + Q_{neu}).$$

The use of the parameter e_{eff} takes into account, in an average way, the effect of core polarization produced by the deformed nature of the nucleus.¹² For simplicity, we assumed that e_{eff} was independent of the various particle-hole pairs contributing to the collective transitions. Experimental infor-

mation for a few transitions in the Pb region¹² show, however, that $e_{eff} = 0.4$ for orbits above the $N = 126$ shell, being about half of $e_{eff} = 0.9$ for those below. In the way we use e_{eff} , it may thus be expected that its value decreases as A increases, which is in fact the case. The values we used, fixed so as to fit the experimental $B(E2; 2_1^+ - 0_1^+)$, were 0.75, 0.72, 0.60, 0.52, 0.56 for ¹⁸⁶⁻¹⁹⁴Os, and 0.92, 0.74, 0.67, 0.58, 0.54, 0.54 for ¹⁸⁸⁻¹⁹⁸Pt.

The formula used to calculate the magnetic moment of the 2_1^+ state was given in Ref. 4, containing no adjustable parameter. The calculation was made in the lowest order, where the magnetic moment operator is simply proportional to the angular momentum operator, hence making all the $M1$ transitions vanish.

III. RESULTS OF CALCULATIONS

A. Energy spectra

In Fig. 1, we plot the energies of the ground- and the γ -band states for ¹⁸⁶⁻¹⁹⁴Os and ¹⁸⁸⁻¹⁹⁸Pt, both experimental and theoretical. The experimental ground-band energies indicate that ¹⁸⁶Os is fairly well deformed and that the deformation decreases as A increases in Os. On the other hand, none of

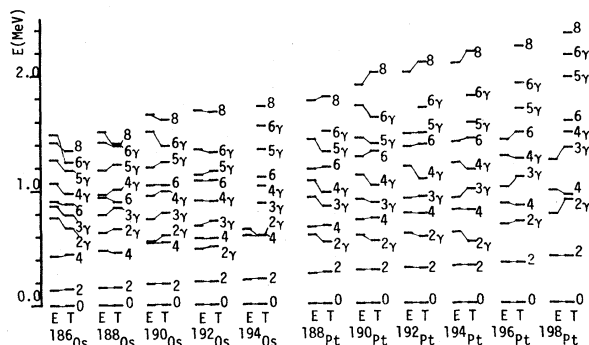


FIG. 1. Comparison of experimental (E) and theoretical (T) energies for the ground- and gamma-band states in ¹⁸⁶⁻¹⁹⁴Os and ¹⁸⁸⁻¹⁹⁸Pt. See Tables II and III for experimental references.

the Pt nuclei is a good rotor, showing that the filling of two of the six proton holes (in Os) decreases the deformation significantly.

It is seen that the theory fits very nicely the ground-band states up to the 8_1^+ state for most of the cases. As regards the γ -band states, we see experimentally that the band-head energy decreases as A increases in Os till ^{192}Os , beyond which it begins to increase again. For Pt, on the other hand, the band-head energy remains nearly constant till ^{194}Pt and begins to increase beyond it. Though the theory does not predict these band-head energies perfectly, it reproduces the above trend. We also note that the spacing between the 2γ and 3γ states increases for both Os and Pt as A increases. Our calculation agrees with this trend, though the splitting is a little too much for ^{194}Pt and ^{196}Pt . This causes the 3γ and 4γ states in these two nuclei to lie somewhat too close together. The designation of the 4_2^+ state in the Pt isotopes as 4_7^+ , however, may be a misnomer.

In Tables II and III, we give a more thorough listing of our predicted energies together with experimentally known energies.¹⁶⁻³⁵ (The latter are given in parentheses, and, for some higher states, the correspondence was made by comparing decay

transitions whenever possible.) Overall, the agreement obtained is seen to be very good. A notable difficulty, which can be found nevertheless, is that the theory predicts the 0_2^+ energy too low. This problem will be discussed in more detail later.

Casten *et al.*^{6,7} emphasized the appearance of $0^+-2^+-2^+$ triads in ^{190}Os and presented a prediction based on IBA (interacting boson approximation).³⁶ In Fig. 2 we present a representative comparison of the IBA (Refs. 7, 16) and BET predictions for the ground- and γ -band states and a $0_2^+-2_3^+-2_4^+$ triad (called $0'-2_1'-2_2'$ for convenience) in these two nuclei. It is seen that BET predicts these energies at least as good as does IBA. It may also be noted that the problem of the $0'$ (i.e., the 0_2^+) energy exists in IBA also.

Casten and Cizewski⁶ further emphasized the appearance of a band in Os which they called the $K=4$ band. In order to show that not only IBA but also BET predicts this band, we compare in Fig. 3 the two predictions with experiment.^{16, 17, 23, 24, 37} It is seen that the two theories are of about the same quality, both predicting somewhat too high the band-head energy, but correctly the spacing(s) between states that belong to this band. Note that

TABLE II. Energies in keV predicted by BET, with the corresponding experimental (Refs. 16-25) energies in parentheses for $^{186-194}\text{Os}$.

	^{186}Os	^{188}Os	^{190}Os	^{192}Os	^{194}Os
0_2	740 (1061)	734 (1086)	748 (912)	677 (956)	724
0_3	1167 (1456)	1215 (1478)	1117 (1545)	964 (1206)	1473
0_4	2038 (1990)	1825 (1704)	2053 (1732)	1991	1521
0_5	2547	2497 (1765)	2745	2603	2351
2_1	145 (137)	156 (155)	186 (187)	206 (206)	226 (219)
2_2	671 (767)	666 (633)	607 (558)	507 (489)	601 (656)
2_3	978	1011 (1305)	1036 (1114)	932	1082
2_4	1153	1243 (1462)	1200 (1435)	1048	1357
2_5	1328	1429 (1807)	1269	1139	1816
2_6	1808	2079	2075	1980	1863
3_1	790 (910)	853 (790)	810 (756)	732 (690)	887
3_2	1287	1390 (1620)	1290	1131	1659
4_1	449 (434)	468 (478)	551 (548)	585 (580)	606 (601)
4_2	978 (1070)	965 (1012)	996 (955)	908 (909)	1040
4_3	1140 (1195)	1271	1243	1143	1366
4_4	1321	1464 (1279)	1383 (1163)	1227 (1070)	1521
4_5	1475 (1321)	1541	1447	1296	1784
5_1	1180 (1276)	1236 (1181)	1246 (1204)	1168 (1140)	1357
5_2	1432	1685 (1516)	1571	1418 (1362)	1747
5_3	1688 (1560)	1762	1653 (1446)	1473	2134
6_1	886 (869)	904 (940)	1053 (1050)	1091 (1088)	1114
6_2	1249 (1491)	1389 (1425)	1391 (1514)	1329 (1360)	1558
6_3	1490	1669	1650	1533 (1465)	1910
6_4	1943	1837	1977 (1836)	1588	2023
7_1	1461	1627	1640	1579 (1713)	1900
8_1	1345 (1421)	1412 (1514)	1623 (1666)	1691 (1708)	1726
10_1	1855 (2069)	1987	2256	2345	2421

TABLE III. Same as Table II but for $^{188-198}\text{Pt}$. Experiment is taken from Refs. 7 and 26-35.

	^{188}Pt	^{190}Pt	^{192}Pt	^{194}Pt	^{196}Pt	^{198}Pt
0_2	692 (798)	736 (921)	832 (1195)	920 (1267)	1021 (1135)	1031 (914)
0_3	1272	1512	1497	1474 (1497)	1375 (1403)	1502 (1480)
0_4	1501	1575	1757	1898 (1547)	2107 (1823)	2378
0_5	2174	2591	2700	2817 (1893)	2774	2560
2_1	281 (266)	298 (296)	314 (316)	329 (328)	352 (355)	411 (407)
2_2	541 (605)	555 (598)	585 (612)	536 (621)	713 (688)	897 (775)
2_3	1020 (1125)	1063 (1203)	1182 (1440)	1291 (1512)	1440 (1362)	1591
2_4	1280 (1312)	1319 (1395)	1484 (1576)	1614 (1622)	1793 (1677)	2000
2_5	1698	1997	1999	2005 (1671)	1928 (1604)	2073
2_6	1992	2044	2269	2444	2390 (1847)	2576
3_1	862 (936)	886 (917)	935 (921)	1001 (922)	1105 (1015)	1356 (1280)
3_2	1639	1661	1871	2018	2241	2578
4_1	688 (671)	748 (738)	785 (785)	817 (812)	853 (877)	944 (985)
4_2	980 (1085)	1038 (1128)	1091 (1201)	1165 (1229)	1261 (1293)	1489 (1428)
4_3	1244	1287	1353	1447	1593	1932
4_4	1461	1529	1674	1798	1973	2231
4_5	1751	1792	1986	2125	2325	2605
5_1	1336 (1443)	1404 (1450)	1488 (1482)	1577 (1499)	1648	1976
5_2	1634	1688	1785	1898	2071	2476
5_3	2250	2295	2522	2657	2861	3216
6_1	1203 (1185)	1328 (1287)	1392 (1365)	1446 (1412)	1489 (1447)	1594 (1713)
6_2	1511	1630 (1732)	1715	1814	1919	2164
6_3	1788	1886	1983	2105	2266	2635
6_4	2012	2092	2241	2375	2582	2935
7_1	1902	2030	2154 (2113)	2268	2399	2698
8_1	1815 (1783)	2023 (1915)	2116 (2018)	2196 (2100)	2243	2349
10_1	2515 (2438)	2816 (2535)	2942 (2518)	3052	3099	3197

in our BET calculations this band head is identified as the 4_4^+ state; see Table II. The fact that $E(4_4^+)$ is somewhat too high is related to the somewhat too low $E(0_2^+)$ mentioned above. A mechanism, to be discussed below, which makes $E(0_2^+)$ too low also brings a 4^+ state, called 4_3^+ in Table II, below the 4_4^+ . A repulsion between the 4_3^+ and 4_4^+ states

then makes $E(4_4^+)$ too high. In other words, if the $E(0_2^+)$ problem were solved, so would that of $E(4_4^+)$.

B. Electromagnetic properties

In Fig. 4, we compare the theoretical quadrupole moment $Q(2_1^+)$ with experiment.^{25,27,38,39} For Os

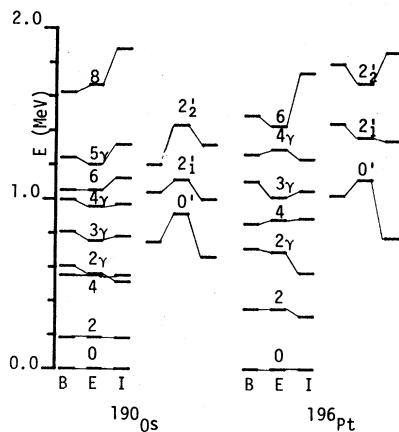


FIG. 2. Comparison of IBA (I) (Refs. 7 and 16), experimental (E) (Refs. 7 and 16), and the boson expansion (B) energies for ^{190}Os and ^{196}Pt . The states $0_2^+-2_3^+-2_4^+$ also called $0_2^+-2_3^+-2_4^+$ in the text.

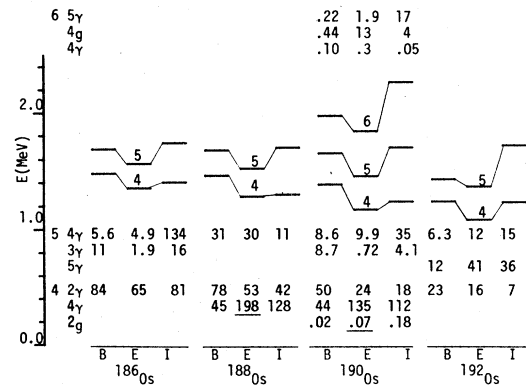


FIG. 3. Same as Fig. 2 except for the $K=4$ bands of $^{186-192}\text{Os}$. Also given are the relative $B(E2)$'s assuming that $B(E2; 4^+ \rightarrow 3_2^+)$, $B(E2; 5^+ \rightarrow 4^+)$, and $B(E2; 6^+ \rightarrow 5^+)$ are equal to 100. Experiment is taken from Refs. 16, 17, 23, 24, and 37, and summarized in Ref. 6. The underlined experimental $B(E2)$'s are upper limits.

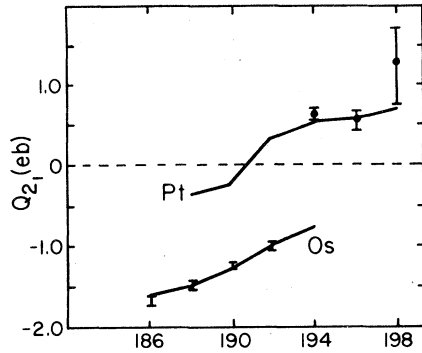


FIG. 4. Comparison of theoretical quadrupole moment for the first 2^+ state (indicated by lines) and experiment (Refs. 25, 27, 38, and 39).

isotopes the agreement is seen to be almost perfect. For Pt the data is less definitive, but it is clear that the sign is opposite to that in Os, and BET reproduces this, fitting the magnitudes as

well. It is also seen that the BET predicts a transition from prolate to oblate in going from ^{190}Pt to ^{192}Pt . Experimental testing of this would be of great interest.

In Table IV, we present various calculated branching ratios, and compare them with available experimental data.^{7, 16-24, 26, 30-34, 40, 41} The overall agreement achieved is remarkable especially when one notes that many of the quantities in question involve $B(E2)$'s which are small, and that some have rather peculiar dependence on N and/or Z . Take as an example the ratio $B(E2; 4_2^+ \rightarrow 3_1^+)/B(E2; 4_2^+ \rightarrow 4_1^+)$. Experimentally this ratio is large for the Os isotopes, while it is rather small for the Pt isotopes, and the theory correctly reproduces this.

Another example of interest is the decay of the 0_2^+ and 0_3^+ states, as pointed out by Casten and Cizewski.⁶ Experiment shows that 0_3^+ decays (predominantly) to the 2_2^+ in $^{188, 190}\text{Os}$, while it goes

TABLE IV. $B(E2; I_i \rightarrow I_f)/B(E2; I_i \rightarrow I_f')$ for the Os and Pt isotopes. The theoretical predictions are on the same line as the transition labeling, while experiment lies directly below, if available. Experiment is taken from Refs. 7, 16-24, 26, 30-34, 40, and 41.

I_i	I_f/I_f'	^{186}Os	^{188}Os	^{190}Os	^{192}Os	^{194}Os	^{188}Pt	^{190}Pt	^{192}Pt	^{194}Pt	^{196}Pt	^{198}Pt
2_2	$0_1/2_1$	0.51	0.38	0.31	0.18	0.16	0.043	0.033	0.0032	2×10^{-5}	0.0019	0.016
		0.43	0.30	0.19	0.11	0.25	0.034	0.012	0.005	0.0038	1×10^{-5}	0.0016
3_1	$4_1/2_2$	0.11	0.13	0.17	0.24	0.26	0.40	0.42	0.39	0.35	0.32	0.26
				0.16				0.50	0.33	0.70	0.95	
3_1	$2_1/2_2$	0.15	0.19	0.18	0.15	0.15	0.085	0.063	0.0055	6×10^{-5}	0.0036	0.025
				0.086	0.088		0.045	0.019	0.0076	0.006	0.0013	
4_2	$2_2/4_1$	2.17	1.85	1.59	1.20	1.41	1.00	0.94	1.08	1.25	1.35	1.53
		2.86	2.32	1.79	1.00			0.74	1.25	0.87	0.92	
4_2	$3_1/4_1$	4.26	3.00	2.25	1.27	1.09	0.14	0.089	0.024	0.18	0.35	0.76
		9.51		1.82	0.81				<0.04		<0.31	
4_2	$2_1/4_1$	0.20	0.18	0.14	0.11	0.085	0.074	0.062	0.023	0.0091	0.0011	0.0074
		0.13	0.07	0.027	0.008			0.006	0.011	0.011	0.017	
5_1	$4_2/3_1$	0.79	0.95	1.08	1.24	0.64	0.55	0.61	0.58	0.57	0.56	0.54
		<1.45			1.67							
5_1	$4_1/3_1$	0.17	0.21	0.21	0.22	0.15	0.13	0.11	0.022	0.003	0.0002	0.019
		0.086	0.061	0.067	0.073							
5_1	$6_1/3_1$	0.14	0.20	0.24	0.37	0.35	0.52	0.56	0.54	0.47	0.41	0.31
		0.15										
6_2	$5_1/4_2$	0.72	0.59	0.64	0.63	0.32	0.086	0.062	0.0084	0.059	0.11	0.23
		1.01										
6_2	$6_1/4_2$	0.28	0.30	0.39	0.59	0.38	0.54	0.58	0.46	0.39	0.35	0.31
		0.16	0.46									
0_2	$2_1/2_2$	0.10	0.17	0.14	0.13	0.23	0.063	0.024	0.0026	0.031	0.12	0.90
			0.21	0.10			>0.11	0.11	0.038	0.078	0.16	
0_3	$2_1/2_2$	7.1	0.003	0.25	0.48	0.24	1.5	0.52	12.5	333	10.5	18.2
			0.18	<0.08						19.2	>19.2	
0_4	$2_1/2_2$	0.32	0.24	0.55	1.08	0.80	0.002	4.90	1.18	0.67	0.26	0.82
			0.24	0.37						1.06	>33.3	

to the 2_1^+ in $^{194,196}\text{Pt}$. On the other hand, the 0_2^+ decays to the 2_2^+ state for all these nuclei except ^{198}Pt . It is again remarkable that BET predicts these features very naturally.

The ratio $B(E2; 2_2^+ \rightarrow 0_1^+)/B(E2; 2_2^+ \rightarrow 2_1^+)$ drops experimentally in Os as mass increases till ^{194}Os , where it increases. Our theory predicts this ratio to decrease, but at ^{194}Os it levels off rather than increase. As will be discussed below, however, this may not be too serious a problem. As regards the Pt isotopes, this ratio is very small, and it is seen in Table IV that BET again predicts this correctly, succeeding in reproducing also the general trend of its dependence on A .

We further remark that the decay properties of states in the $K=4$ bands are presented in Fig. 3. It is seen again that good agreement with experiment was obtained, showing that BET predicts properties of states even with such high excitation energies.

In Table V, we list the ratios of $B(E2)$'s (multiplied by a factor of 100) for the 2^+ states of the $0^+-2^+-2^+$ sequences for $^{188,190}\text{Os}$ and $^{194,196}\text{Pt}$. Experiment indicates that for the $0_2^+-2_3^+-2_4^+$ sequence, the 2_3^+ state decays to the 0_2^+ state very strongly and to the 3_1^+ state fairly strongly, all other decays being weak. The 2_4^+ decays most strongly to the 2_3^+ . For the $0_3^+-2_5^+-2_6^+$ sequence in ^{196}Pt , only the intra-sequence transitions are strong. Our results agree rather well with the data. The nature of these sequences will further be elucidated in the next section.

In Table VI, we present absolute $B(E2)$'s, magnetic and quadrupole moments of the 2_1^+ states for all the Os-Pt nuclei. If we consider just the theoretical trends in Table VI, we observe the weakness of the $4_2^+ \rightarrow 3_1^+$ transition in Pt, with both it and the $0_2^+ \rightarrow 2_1^+$ having minima at ^{192}Pt , and their enhancement for ^{198}Pt . The increased $2_2^+ \rightarrow 2_1^+$ transition for Pt as opposed to Os is also seen. Experimentally, the $2_2^+ \rightarrow 2_1^+$ behavior is known extensively and the BET prediction agrees quite well with experiment. In addition, the sudden increase in $B(E2; 0_2^+ \rightarrow 2_1^+)$ for ^{198}Pt was confirmed by the recent experiment by Bolotin and his co-workers.²⁶ We further note that for ^{194}Os we predict that the $2_2^+ \rightarrow 2_1^+$ transition decreases suddenly, and this is consistent with the observed increase of $B(E2; 2_2^+ \rightarrow 0_1^+)/B(E2; 2_2^+ \rightarrow 2_1^+)$ for this nucleus. The inability of our calculations to predict this ratio's increase may then be traced to the prediction of $B(E2; 2_2^+ \rightarrow 0_1^+)$. Overall, Table VI shows that data is still scarce and its accumulation is needed, including the measurement of the absolute values of $B(E2; 2_2^+ \rightarrow 0_1^+)$ and $B(E2; 2_2^+ \rightarrow 2_1^+)$ in ^{194}Os .

Regarding the magnetic moments for the 2_1^+ states, the agreement obtained can be said to be very good, considering that no adjustable parameter was involved in their calculation.

An interesting experimental measurement is that of the sign⁴⁹ of the Coulomb interference term P_4 , defined by $P_4 = M(2_1^+, 2_1^+) M(2_2^+, 2_2^+) M(2_1^+, 0_1^+) M(2_2^+, 0_1^+)$, where M is the $E2$ matrix element taken between the states given as arguments. For $^{186-192}\text{Os}$,

TABLE V. $10^2 \times B(E2; I_i \rightarrow I_f) / B(E2; I_i \rightarrow I_{f'})$ for the $0_2-2_3-2_4$ and $0_3-2_5-2_6$ sequences for $^{188-190}\text{Os}$ and $^{194-196}\text{Pt}$. Experiment is taken from Refs. 7, 16, 21, and 34.

I_i	$I_f/I_{f'}$	^{188}Os		^{190}Os		^{194}Pt		^{196}Pt	
		BET	EXP	BET	EXP	BET	EXP	BET	EXP
2_3	$3_1/0_2$	68.6	20	64	37	85.8	22	106	60
	$4_1/0_2$	9.9	2	7.0	1.3	0.99	1.6	4.8	2.4
	$2_2/0_2$	0.11	<1.5	0.74	<0.2	1.0	1.0	2.0	10.0
	$2_1/0_2$	0.25	1.3	0.26	0.9	0.2	1.5	0.34	1.1
	$0_1/0_2$	1.30	0.13	0.49	0.2	0	0.3	0.08	
2_4	$0_2/2_3$	14.4		31.8	6.2	0.23		0.002	9.0
	$3_1/2_3$	10.0		22.5	3.0	1.2		1.2	9.0
	$4_1/2_3$	0.05		0.78	3.8	0.32		1.9	1.5
	$2_2/2_3$	0.48		0.38	1.1	0.38		1.7	2.1
	$2_1/2_3$	0.30		0.004	0.6	0.18		0.17	1.4
	$0_1/2_3$	0.11		0.06	0.3	0		0.04	0.7
2_5	$3_1/0_3$	4.4		2.3		1.9		0.3	0.4
	$4_1/0_3$	0.4		0.05		28.8		34.2	1.7
	$2_2/0_3$	0.06		0.17		13.4		14.3	0.5
	$2_1/0_3$	0.005		0.008		1.3		1.6	0.26
	$0_1/0_3$	0.20		0.06		1.6		1.5	0.01
2_6	$2_2/2_5$	1.7		0.55		0.35		0.45	0.2
	$2_1/2_5$	0.01		0		1.0		0.95	1.0

TABLE VI. $B(E2; I_i \rightarrow I_f)$ in units of $10^{-2}e^2b^2$, electric quadrupole and magnetic dipole moments for the 2_1^+ state in units of $e b$ and μ_N , respectively. Experiment, with error in parentheses, is given below the theoretical prediction. Experimental $B(E2)$'s are taken from Refs. 26–29, 37, and 42; while the μ_N are taken from Refs. 43–48. See Fig. 4 for the quadrupole moment references. An asterisk denotes that the 3^+ spin assignment is uncertain.

I_i	I_f	^{186}Os	^{188}Os	^{190}Os	^{192}Os	^{194}Os	^{188}Pt	^{190}Pt	^{192}Pt	^{194}Pt	^{196}Pt	^{198}Pt
2_1	0_1	65.1	56.5	47.9	41.3	33.3	48.1	45.0	40.0	33.2	27.3	21.2
		64.2(57)	55.6(30)	47.4(25)	39.8(22)		52.0(9)	49.0(14)	37.8(6)	32.4(3)	26.4(11)	20.9(19)
4_1	2_1	95.9	84.7	72.0	61.6	51.7	72.7	66.8	60.0	50.9	43.3	36.3
		83.7(117)	81.7(87)	66.1(67)	53.9(67)				58.0(30)	44.9(22)	40.9(22)	27.0(18)
6_1	4_1	107.0	95.4	80.0	67.4	61.1	87.3	79.4	72.8	62.1	53.6	46.6
		83.7(117)	116(18)	104(16)	87(17)				47.0(18)		42.1(116)	>39.5
0_2	2_1	4.8	9.8	6.8	5.5	10.0	4.9	1.6	0.15	1.4	4.7	20.2
			3.1(8)								2.2(10)	17.1(41)
0_2	2_2	46.6	56.8	48.8	42.9	42.7	77.8	67.4	56.3	45.5	38.8	22.4
											14.2(77)	
2_2	2_1	17.3	21.3	24.2	33.6	28.4	74.4	69.8	56.7	41.1	31.9	22.8
		8.2(12)	15.6(11)	27.0(20)	32.8(37)				52.0	42.3(15)	31.8(23)	31.2(45)
3_1	2_2	98.5	78.8	70.3	61.3	45.9	67.3	61.6	58.7	49.5	41.1	31.7
												12.0(50)*
3_1	2_1	15.6	14.7	12.5	9.3	7.1	5.7	3.9	0.33	0.003	0.15	0.80
												0.28(12)*
4_2	4_1	18.4	20.3	20.7	23.5	20.1	44.4	40.4	31.9	23.2	18.3	13.5
		17.6(53)	15.9(32)	36.2(72)	36.7(184)					87(43)	19.3(97)	
4_2	2_2	40.0	37.5	33.0	28.3	28.4	44.3	38.1	34.5	29.0	24.8	20.7
		55(19)	58(19)	49(10)	17(3)					69.0(39)	17.7(25)	>67.8
4_2	3_1	78.4	60.9	46.6	29.8	21.9	6.2	3.6	0.76	4.1	6.3	10.2
4_2	2_1	3.7	3.6	3.0	2.6	1.7	3.3	2.5	0.74	0.21	0.028	0.10
		1.4(4)	1.1(2)	1.0(2)						1.0(5)	0.3(1)	
5_1	3_1	61.4	49.7	40.7	31.2	34.6	50.4	44.9	42.3	36.5	31.6	26.5
2_3	0_2	59.5	41.1	35.0	25.7	27.7	40.1	37.2	32.7	27.2	22.3	18.4
μ_{2_1}		0.801	0.794	0.806	0.827	0.860	0.709	0.707	0.710	0.737	0.775	0.843
		0.48(10)	0.58(6)	0.78(6)	0.78(6)				0.685(75)	0.698(62)	0.66(8)	0.64(16)
		0.562(16)			0.797(36)				0.90(11)	0.640(60)		
Q_{2_1}		-1.61	-1.46	-1.28	-1.01	-0.90	-0.36	-0.22	0.36	0.54	0.58	0.65
		-1.65(4)	-1.47(4)	-1.18(3)	-0.99(3)					0.63(6)	0.56(18)	1.22(50)

$P_4 < 0$, while for $^{192-196}\text{Pt}$, $P_4 > 0$. We predict $P_4 < 0$ for all the isotopes in this study except for ^{192}Pt . A similar result has been found by Kumar.⁵⁰ Among the four M factors appearing in P_4 , the $M(2_2^+, 0_1^+)$ is rather small for some of the Pt isotopes, due to strong cancellations in its calculation. In particular for ^{194}Pt , we predict the corresponding $B(E2)$ to be $8.2 \times 10^{-6} e^2 b^2$, as can be derived from Tables IV and VI. Since this $B(E2)$ tests fine details of the wave functions, which we would be lucky to predict perfectly, we can be satisfied with showing that $P_4 > 0$ can be predicted with our theory; note that, e.g., the simple asymmetric rotor model always predicts⁵¹ $P_4 < 0$. We may further remark that we predicted $Q(2_2^+)$ to be

nearly equal in magnitude and opposite in sign to $Q(2_1^+)$ for $^{192-196}\text{Pt}$. This indicates that the 2_2^+ is indeed a 2_2^+ type state, and thus that no large changes in structure are necessary to occur for P_4 to switch sign. The calculations of Baker⁴⁹ suggest that the inclusion of the effects of hexadecapole deformation might be important to obtain the sign of P_4 correctly. In our terminology, this might mean that it is desirable to extend our scheme slightly by adding the hexadecapole-hexadecapole type force in our calculation as a new term in our effective interaction. This may affect the $B(E2; 2_2^+ \rightarrow 0_1^+)$ in the Os isotopes also, so that the branching ratio discussed earlier may increase at ^{194}Os .

A significant feature of our calculations has been

the correct prediction of quadrupole moments $Q(2_1^+)$, including sign, for the Os-Pt isotopes. To show that this was not achieved by our use of parametrization, we present in Table VII a comparison between the results previously given and those from a calculation in which we have fixed f_2 , g_2 , e_{eff} , and the $i_{13/2}$ single-particle energy. We see that $E(2_1^+)$, $B(E2; 2_1^+ \rightarrow 0_1^+)$, and $Q(2_1^+)$ predictions are not altered greatly except for a few cases. In particular, the shape transitions remain unchanged with the fixed parameters. All other features, such as branching ratios, are also qualitatively unchanged.

One last topic is the decay of higher 0^+ states as emphasized by Casten and Cizewski.⁶ We feel that this emphasis is premature. As one can see in Table IV, the decay of the 0_4^+ state varies quite a bit in our calculations for the Pt isotopes. This is because most of the $B(E2)$'s involved are very small, especially for the Pt isotopes. In Ref. 6, the IBA calculations disagreed with the experimental branching ratios for the 0_4^+ states for ^{194,196}Pt. We might then interpret our result for ¹⁹⁴Pt (see Table IV) to be fairly significant. However, we have calculated⁵² the energies of two-

quasiparticle 0^+ states and found them to lie at roughly 2 MeV in excitation, i.e., just above the experimental positions of the higher 0^+ states and in between our 0_4^+ and 0_5^+ collective state calculations. The correct physical description of these experimental states must thus include coupling with these other degrees of freedom. In these isotopes, where the theoretical $B(E2)$'s for these transitions are of single-particle magnitude or less, the agreement of these particular branching ratios with experiment, achieved with purely collective theories, is not significant.

C. Potential energy surfaces

Starting with the boson Hamiltonian used in the calculations presented above, it is possible to make a transformation² to conjugate variables β_μ and π_μ of the Bohr-Mottelson model.⁸ The part depending exclusively on β_μ is called the potential energy part and it can further be expressed in terms of the variables β and γ , again of the Bohr-Mottelson model. We shall call this $V(\beta, \gamma)$. Its explicit form was given in Ref. 2, when the Hamiltonian was terminated at the fourth order. Here, we give its form for the sixth order case:

$$V(\beta, \gamma) = c_2\beta^2 + c_3\beta^3 \cos(3\gamma) + c_4\beta^4 + c_5\beta^5 \cos(3\gamma) + [c_6 + c_7 \cos^2(3\gamma)]\beta^6, \quad (1)$$

where

$$\begin{aligned} c_2 &= z^{-2} [h_{11} - 3h_{22N} - 3.5h_{31} - 6h_{22J} + h_{22V} - h_{22P} \\ &\quad + (17h_{601} + 25h_{511} + 33h_{421} + 59h_{422})/4 + 21h_{423} + 15h_{333} + 2h_{424} + (143h_{332} - 5h_{331})/8], \\ c_3 &= (z^{-3}/\sqrt{7}) [h_{21} + h_{30} + h_{411} + 2h_{321} - 4h_{412} - 3(h_{322} + h_{323})], \\ c_4 &= (z^{-4}/4) [2h_{31} + h_{22N} + h_{22P} + 2h_{40} - 9h_{511} - 8h_{421} - 16h_{422} - 12h_{423} - 6.5h_{331} - 10.5h_{332} - 6h_{333} - (\frac{2}{7})h_{424}], \\ c_5 &= (z^{-5}/2\sqrt{7}) (h_{411} + h_{501} + h_{412} + h_{321} + h_{322} + h_{323}), \\ c_6 &= (z^{-6}/4) [h_{601} + h_{511} + h_{421} + h_{422} + (h_{331} + h_{332})/2], \\ c_7 &= (z^{-6}/14) [h_{602} + h_{512} + h_{425} + h_{424} + (h_{334} + h_{335})/2]. \end{aligned} \quad (2)$$

TABLE VII. Comparison of the energy $B(E2; 2_1^+ \rightarrow 0_1^+)$ and quadrupole moment for the 2_1^+ state, between our usual calculations and one where we fix $\chi_2 = 0.036$ MeV, $G_2 = 0.026$ MeV, and $e_{\text{eff}} = 0.70$, and the single particle energy of the $i_{13/2}$ state is set at its value for $A = 192$.

	¹⁸⁶ Os	¹⁸⁸ Os	¹⁹⁰ Os	¹⁹² Os	¹⁹⁴ Os	¹⁸⁸ Pt	¹⁹⁰ Pt	¹⁹² Pt	¹⁹⁴ Pt	¹⁹⁶ Pt	¹⁹⁸ Pt
E_{2_1}	145	156	186	206	226	281	298	314	329	352	411
$E_{2_1}^{\text{fix}}$	101	95	180	206	80	304	359	503	492	378	527
$B(E2; 2_1 \rightarrow 0_1)$	0.651	0.565	0.479	0.413	0.333	0.481	0.450	0.400	0.332	0.273	0.212
$B(E2; 2_1 \rightarrow 0_1)^{\text{fix}}$	0.588	0.547	0.479	0.472	0.499	0.370	0.368	0.350	0.350	0.387	0.316
Q_{2_1}	-1.61	-1.46	-1.28	-1.01	-0.90	-0.36	-0.22	0.36	0.54	0.58	0.65
$Q_{2_1}^{\text{fix}}$	-1.58	-1.53	-1.28	-1.11	-1.49	-0.41	-0.25	0.22	0.39	0.80	0.90

In (2) the quantities h_{mni} were defined in Ref. 2. The h_{mni} is a coefficient in the boson Hamiltonian of a term of the order $m+n$, i.e., a term containing m creation and n annihilation operators, the index i discriminating between terms that have the same pair of m and n . The convergence of the boson expansion we discussed in Sec. II guarantees that h_{mni} with larger $m+n$ are much smaller in magnitude compared with those with smaller $m+n$. The following discussion is essentially unaffected by consideration of h_{mni} with $m+n > 4$.

In (1) it is clear² that the signs of c_3 and c_5 indicate whether the nucleus is predicted to be predominantly prolate or oblate. It is also obvious that $c_6 + c_7 \cos^2(3\gamma)$ must be positive, because otherwise the nucleus collapses to an infinite deformation. For the details of the collective behavior of the nucleus, one must include the effects of the terms that include π_μ . (The boson Hamiltonian, of course, does this.) The consideration of $V(\beta, \gamma)$ alone, nevertheless, gives a good insight into what is taking place in individual nuclei.

In Fig. 5 we show $V(\beta, \gamma)$ in the limits of $\gamma = 0^\circ, 60^\circ$, which, as is well known, correspond respectively to prolate and oblate deformations with an axial symmetry. It is convenient, for the following discussion, to call V_{dif} the difference between the depths of the well minima in prolate and oblate sides of each figure; $V_{\text{dif}} = |V_{\text{pro}}| - |V_{\text{ob}}|$.

Considering Os isotopes first, we find that $V_{\text{dif}} > 0$, and as mass increases, $|V_{\text{dif}}|$ as well as the equilibrium value for β decreases. This bears out the quantitative behavior of the quadrupole moment calculations seen in Fig. 4. For the Pt isotopes, on the other hand, we have $V_{\text{dif}} < 0$ throughout, though $|V_{\text{dif}}|$ is very close to zero for $^{188, 190}\text{Pt}$, while taking somewhat larger but nearly A independent values for $^{192-198}\text{Pt}$.

As we remarked above, c_3 and c_5 are responsible for determining the value of V_{dif} . We shall now proceed to the discussion of the roles played by other coefficients in determining the shapes of the potential energy surfaces.

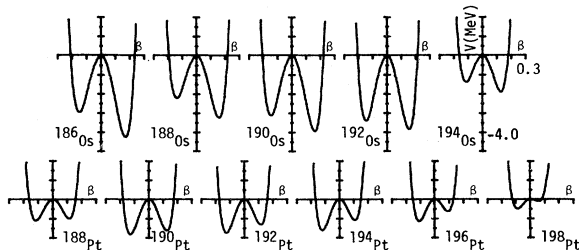


FIG. 5. Potential surface plots for the Os and Pt isotopes. Right (left) side corresponds to $\gamma = 0^\circ$ (60°).

First of all, that $V(\beta, \gamma)$ is peaked at $\beta = 0$, i.e., that potential wells are formed, is due to the fact that $c_2 < 0$, which in turn is a consequence of the fact that BET predicts for Os-Pt nuclei rather large anharmonicity, more precisely, rather large fourth order terms. Take a look at the expression for c_2 in Eq. (2). The h_{11} is the coefficient of the boson operator $(\alpha_2^+ \alpha_2)_0$, while h_{31} and h_{22N} are the coefficients of the operators $(\alpha_2^+ \alpha_2^+)_0 (\alpha_2^+ \alpha_2)_0 + \text{H.c.}$ and $(\alpha_2^+ \alpha_2)_0 [(\alpha_2^+ \alpha_2)_0 - 1]$, respectively, in the boson Hamiltonian. The latter two coefficients become comparable to h_{11} after the unitary transformation is made so as to make $h_{20} = 0$; see Ref. 2. If $3h_{22N} + 3.5h_{31}$ exceeds h_{11} significantly, it is obvious that we get $c_2 < 0$, making the $\beta = 0$ point a local maximum, irrespective of the presence of the c_3 and c_5 terms. If indeed $3h_{22N} + 3.5h_{31} \gg h_{11}$, and further $c_3 = c_5 = 0$, the system loses any preferential value of γ , having the same equilibrium β for any γ . This is nothing but a manifestation of the γ -unstable model of Wilets and Jean.⁵

That model predicts various characteristic features in the resultant spectrum, but two of them may be the most conspicuous. One is that the energy of the 0_2^+ state appears very high,⁵ and the other is that the 3_1^+ and 4_2^+ states lie close together.⁵³ Of course the presence of other terms in (1), as well as of terms involving the π_μ operators, prevents the actual nuclei from having this ideal limit. Nevertheless, the Os-Pt nuclei have in various ways the features which this model predicts, as we have seen above.

At this point we want to point out an example which warns us against taking the potential energy surfaces of Fig. 5 too literally. Based on this figure, one would tend to conclude that $^{188, 190}\text{Pt}$ are oblate. Our calculation, including all the dynamics of the system, however, predicted negative $Q(2_1^+)$ for these two nuclei, showing that they behave as if they were prolate.

We now show an example in which the potential energy surface in Fig. 5 gives a clue to understanding the somewhat peculiar behavior of ^{198}Pt . It is seen that the potential energy surface for ^{198}Pt has lost its prolate well, only the well in the oblate side remaining. This suggests that the γ -unstable nature, which exists in lighter Pt isotopes to various degrees, should disappear in ^{198}Pt . That this is, in fact, the case can be seen clearly from what we gave in Fig. 2 and Tables III-V. Note in particular that $E(0_2^+)/E(2_1^+) = 2.25$ in ^{198}Pt . Also the spacing between the 2_2^+ and 3_1^+ states is rather large in ^{198}Pt , making these two states look less like members of a γ band. In fact ^{198}Pt behaves more like a spherical nucleus. All these features are implied by Fig. 5.

We have discussed above the significance of large h_{31} and h_{22N} coefficients in resulting in γ -unstablelike spectra. We shall now discuss its consequence on the transition probabilities. Each of the basis states within which our boson Hamiltonian is diagonalized may be denoted by $(N, v)_I$, where N is the number of (collective) bosons, I is the spin, and v is the seniority, i.e., the number of bosons not paired to angular momentum zero. Somewhat crudely speaking, the role which the operators multiplied by h_{31} and h_{22N} play is to push up states (dominated by) $(N, N-2)_I$ relative to the states (dominated by) $(N+1, N+1)_I$.

In Fig. 6, we present a schematic spectrum where the dominant component (or the major component for the higher states) is labeled for each state in a γ -unstablelike nucleus such as ^{196}Pt . Noting that the strong $E2$ transitions take place by changing the boson number N by one unit, it is easy to see from Fig. 6 why, in nuclei like ^{194}Pt and ^{196}Pt , the 0_2^+ and 0_3^+ states decay preferentially to the 2_1^+ and 2_2^+ states, respectively. Figure 6 also explains very clearly why the 4_2^+ ($=4_2^+$) state decays preferentially to the 4_1^+ rather than to the 3_1^+ ($=3_1^+$) state, making it less meaningful to speak of the 4_2^+ state as the 4_2^+ in the Pt isotopes.

The peculiar decay properties of states in the $0_2^+-2_3^+-2_4^+$ triad is also easy to understand by noting that their major components are $(3, 3)_0$, $(4, 4)_2$,

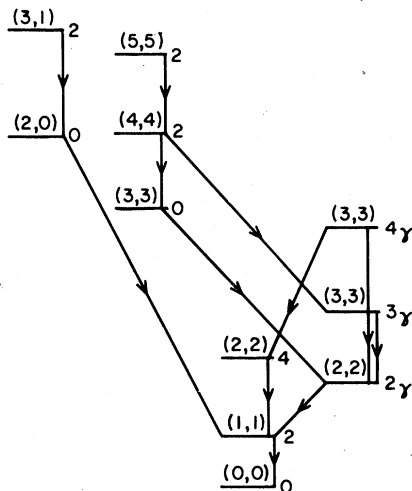


FIG. 6. Schematic decay pattern for $^{192-196}\text{Pt}$ like isotopes. Spin is labeled to the right of each energy level while the (N, v) boson basis state, which is the major component of the nuclear wave function, is labeled above the level. Lines with arrows indicate strong decays. The $0-2-2$ sequence is also called $0_2-2_3-2_4$ while the $0-2$ is called 0_3-2_5 when referring to actual nuclei in the text.

and $(5, 5)_2$, respectively. We have already discussed the 0_2^+ decay to the 2_2^+ state. Similarly, 2_3^+ decays to the 3_1^+ as well as to the 0_2^+ . On the other hand, for the 2_4^+ state, with its $(5, 5)$ character, the easiest way to decay is to the 2_3^+ state with the $(4, 4)$ character.

The $0_3^+-2_5^+-2_6^+$ sequence has for the most part $(2, 0)_0$, $(3, 1)_2$, and $(4, 2)_2$ character, respectively, in ^{196}Pt . The overly enhanced branching of the 2_5^+ to the 4_1^+ and 2_2^+ states, predicted by our calculations (Table V), is caused by a 25% admixture of the $(5, 1)_2$ component in the 2_5^+ state, which has fairly strong overlap with the $N=4$ components in the 4_1^+ and 2_2^+ , and adds coherently to the $N=3$ to $N=2$ overlap. This is also a reason why the energy of this state is predicted to be too high. Since the experimental energies for these states are relatively high, it is likely that coupling to two-quasiparticle states is needed to push down the energies and thus compress the sequence. Presumably this will also affect the relative $B(E2)$'s, since the absolute $B(E2)$'s are not large, and improve agreement with experiment.

The Os isotopes are similar in nature to the example in Fig. 6, but the presence of larger deformation alters that simple picture. These isotopes have more anharmonicity than Pt, making the 0_1^+ the first 0^+ state with significant $(2, 0)$ component. The 0_2^+ and to a lesser extent the 0_3^+ states have $(3, 3)_0$ dominance. Thus both 0_2^+ and 0_3^+ decay to the 2_2^+ rather than to the 2_1^+ ; see Table IV. That the 0_1^+ happens to decay to the 2_2^+ rather than to the 2_1^+ is the result of subtle cancellations which may not be so significant, as pointed out at the end of the previous section. The $N=3$ component is still the major component of the 4_2^+ state, as was the case for Pt, but the presence of greater deformation for the Os isotopes decreases the $(2, 2)_4$ nature of the 4_1^+ state and enhances that component in the 4_2^+ state, thus explaining the larger branching to the 3_1^+ and 2_1^+ states as seen in Table IV.

As regards the $0_2^+-2_3^+-2_4^+$ sequence, the picture is very similar to the Pt case. However, the energies of these states are not predicted very well in ^{190}Os , and this reflects itself into overestimating the $B(E2; 2_4^+ \rightarrow 0_2^+)$ and $B(E2; 2_4^+ \rightarrow 3_1^+)$ in Table V. Note that in ^{188}Os , where the energy spacings within the sequence are closer to experiment than in ^{190}Os , these relative $B(E2)$'s have been reduced.

We once again point out that the γ -unstablelike picture of Fig. 6 completely disappears in ^{198}Pt . This is more clearly seen by the complete transition of the 0_2^+ state, from $N=3$ to predominantly $N=2$ nature, and the resulting increase in $B(E2; 0_2^+ \rightarrow 2_1^+)$ (see Table VI).

A last point concerns quadrupole moment predictions for higher states. For all nuclei considered here, our calculations predict that $Q(2_2^+) = -Q(2_1^+)$ is approximately true. If we consider the 2_2^+ , 3_1^+ , 4_2^+ , 5_1^+ , and 6_2^+ states to form a γ band built on the rotations of an intrinsic $K=2$ state then¹²

$$Q(I) = \frac{3K^2 - I(I+1)}{(I+1)(2I+3)} Q_0^K. \quad (3)$$

Thus we expect that $Q(3_1^+) = 0$, $Q(4_2^+) = -0.5Q(2_2^+)$, $Q(5_1^+) = -0.8Q(2_2^+)$, and $Q(6_2^+) = -Q(2_2^+)$. We find that the 3_1^+ state relation holds exactly in all cases while only for the Os isotopes are the other relations approximately valid. For the Pt isotopes the deviations from the above relations for the 4_2^+ , 5_1^+ , and 6_2^+ states are in some cases fairly large. In particular, $-0.15 < Q(4_2^+) < -0.02$ for ¹⁹²⁻¹⁹⁸Pt, which besides being small has the sign opposite to what Eq. (3) suggests. This is more evidence that the designation γ band in the Pt isotopes is somewhat of a misnomer. Higher energy states for one reason or another cannot be interpreted as the 4_2^+ , ..., etc., members of the γ band. Thus the termination of the usual γ -band picture at the 4_2^+ state is a nontrivial aspect of γ -unstable-like nuclei. Experimental information on the quadrupole moments of higher excited states in both Os and Pt is needed.

Summarizing, we found that both the Os and Pt isotopes are characterized by a γ -unstable nature, though the former, particularly the lighter Os isotopes, are more deformed. To further visualize the difference between the isotopes, we plot in Fig. 7 three branching ratios: $R_1 = B(E2; 4_2 \rightarrow 2_2/4_1)$, $R_2 = B(E2; 4_2 \rightarrow 3_1/4_1)$, and $R_3 = B(E2; 2_2 \rightarrow 0_1/2_1)$. As seen from the discussion on Fig. 6, it is to be expected that $R_2 = R_3 = 0$ if an ideal γ instability is established. The fact that R_2 and R_3 are much smaller for Pt than for Os reflects this. For both deformed and γ -unstable nuclei, R_1 is expected to be close to unity. For a deformed nucleus, $R_2 \gg 1$ because it is the ratio of an intraband over an interband transition, while $R_3 \approx 1$ because it is the ratio of two interband transitions. These facts explain the behavior of the R_2 and R_3 values for Os in Fig. 7

An extremely interesting feature is that for Pt both R_2 and R_3 hit a minimum as functions of N , the neutron number. The number N , where this minimum takes place, may indicate the nucleus at which the transition from a prolatelike γ instability to an oblatelike γ instability is to be expected. In Fig. 4, we saw (theoretically) that this transition takes place at ¹⁹²Pt, while experiment implied that it occurs before ¹⁹⁴Pt. The theoretical R_2 in Fig. 7 also shows that it takes place at

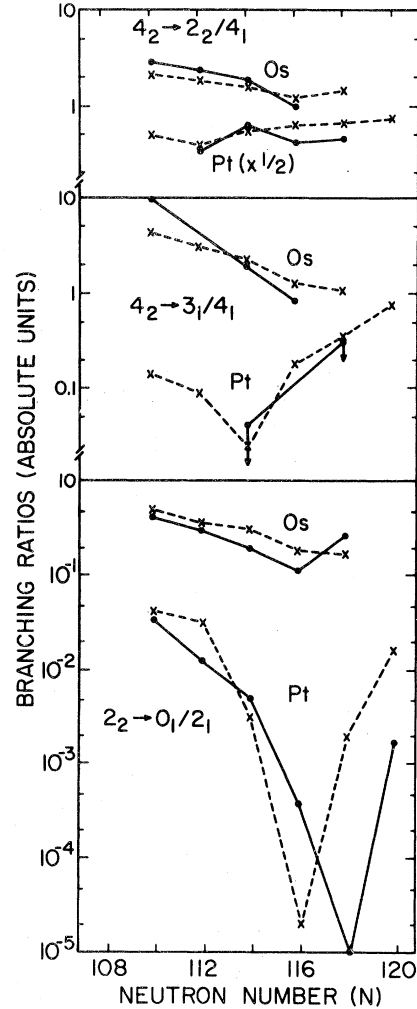


FIG. 7. Ratio of $B(E2)$'s selected from Table IV. Crosses denote theory whereas circles refer to experiment. Arrowed circles denote upper limits.

¹⁹²Pt, which is consistent with the limited data. The experimental (theoretical) R_3 in Fig. 7 indicates that the transition takes place at ¹⁹⁶Pt (¹⁹⁴Pt). This shape change discrepancy is, as discussed earlier, related to the extremely sensitive nature of the $2_2 - 0_1$ transition which is being affected by more than just the quadrupole shape change. Of course, more experimental data in Figs. 4 and 7 would make the situation clearer.

IV. COMPARISON WITH OTHER THEORETICAL WORK AND DISCUSSIONS

Some time ago, Kumar and Baranger (KB) (Ref. 54) formulated a way to describe properties of collective even-even nuclei and analyzed the then available data. The analyses included Os-Pt nuclei and a good fit to data was obtained in general.

In the light of more data which became available later, however, KB theory seems to encounter difficulties in various aspects, notably concerning the decay of the 0_2^+ state; see the item (vii) enumerated in the Introduction. A possible source of trouble in KB theory may be its use of the adiabatic approximation.

Both KB (Ref. 54) and Götz *et al.*⁵⁵ calculated the potential energy surfaces for Os-Pt nuclei, the latter authors using the method of Strutinski.⁵⁶ The results they obtained are very similar to ours presented in Fig. 5. In particular, Götz *et al.* predicted that the sign of deformation should change at ¹⁹²Pt in agreement with our result. (The energy surface of Götz *et al.* includes, in our terminology, the contributions of terms including the π_μ operators. This was possible because their method also uses an adiabatic approximation, though different from that in KB. Götz *et al.* did not discuss how to use their energy surfaces to predict other properties of these nuclei.) They also predicted the absence of the prolate well in ¹⁹⁸Pt with which we agree. However, both KB and Götz *et al.* predicted that ¹⁹⁴Os is oblate, contradicting our result. We note here that our preliminary calculations for ¹⁹⁶Os indicate that it is oblate. Overall, we may say that all three *microscopic* theories are in good accord among themselves.

A good fit to a number of data in Os-Pt nuclei were presented recently by Casten and Cizewski.⁶ The theoretical framework they used was the O(6) limit of the IBA,³⁶ and we have compared above some of their predictions with ours as well as with experiment. From what we have shown, it may be fair to say that the quality of fit to data achieved by IBA and BET is about the same. To some extent, this is not surprising. We have emphasized above that the microscopic theories, our BET and those in Refs. 55 and 56, all predict γ -unstable nature for nuclei in this mass region, and it is well known that the O(6) limit of IBA is very much the same as is the γ -unstable model.

A serious problem which the work in Refs. 6 and 7 encountered is that perhaps because of their emphasis of the O(6) limit, the $Q(2_1^+)$ was predicted to be very small for the Pt nuclei. Furthermore the A dependence of $Q(2_1^+)$ was apparently wrong even if its very small magnitude is accepted. The parameters were chosen so that $Q(2_1^+)$ for the Pt isotopes would decrease as A was increased, reaching close to zero at ¹⁹⁶Pt, in clear contradiction with experiment.

A trouble intrinsic to the phenomenological approach like IBA is that a choice of drastically different sets of parameters sometimes has to be made arbitrarily. Examples are the Os and Pt parameters in Ref. 6 as well as the transition

away from the γ -unstable nature of ¹⁹⁶Pt which occurs at ¹⁹⁸Pt. Also the shift in sign of the quadrupole moment must be introduced by parameter change. More refined parametrizations which make a distinction between proton and neutron bosons were presented by Scholten⁵⁷ for the Os isotopes. The results for energies are an improvement over Ref. 6. However, a comparison between the choice of the parameters of the proton and neutron boson quadrupole operators, which were needed to fit the Os data and microscopic estimates⁵⁸ of the sign of these parameters based on an assumed $j = \frac{3}{2}$ single level degenerate closed shell, were contradictory. As Scholten mentions,⁵⁷ this problem probably arises since the single particle levels in a real nuclear closed shell are not degenerate.

Another phenomenological approach reported recently is that of Hsu *et al.*,⁵⁹ who used a modified version of the rotation-vibration coupling model to fit quite well the energies of ¹⁹⁶Pt; however, it should be remarked that as many as seven free parameters were used. The predictions of $B(E2)$'s were fair in general, but that of the branching ratios of the 0_2^+ decay were very poor. Yadav *et al.*⁶⁰ also used an extended version of the asymmetric rotor model, obtaining good results for the ground- and γ -band energies for ¹⁹⁰Os and ¹⁹⁰Pt, and $B(E2)$'s in ¹⁹⁴Pt.

V. CONCLUDING REMARKS

It was shown that the BET can be applied very nicely for the Os-Pt isotopes. The present work has emphasized the competition of the oblate nature of the proton holes versus the prolate-oblate nature of the neutron holes. It produces nuclei which range from fairly well prolate-deformed to prolate but γ -unstablelike Os isotopes, and from prolate γ unstable to oblate γ unstable and then mildly oblate Pt isotopes. Very good agreement to energies, transition probabilities, and quadrupole as well as magnetic moments were obtained. All of the characteristic features itemized in the Introduction were capable of being understood from the present results. Similarities with the results of other microscopic approaches were also pointed out. We may thus conclude that the physical assumptions¹¹ underlying our calculations were well justified in this mass region.

There exist many possibilities regarding ways to improve our results further. For example, we have quite accurately predicted the decay of the 0_2^+ state, but its energy was somewhat too low. An easy method to get much better results for this energy is the following. Since our quadrupole moments are predicted very nicely, the deformation

being produced by the h_{21} and h_{30} terms must be close to correct. From Eq. (2) we see that the deformation will not change much if we freely decrease h_{21} and increase h_{30} such that $h_{21} + h_{30} = \text{constant}$. The increased h_{30} [coefficient of the operator $(\alpha_2^+ \alpha_2^+ \alpha_2^+) + \text{H.c.}$] then pushes up the 0_2^+ state since $(3, 3)_0$ is its main component. The same adjustment in these two coefficients has been found to work very well for ^{190}Os and ^{194}Pt . That this was a small change in the Hamiltonian was verified by noting that the new f_2 and g_2 that was needed to fit the 2_1^+ energy varied by only 2% from the old, that the position of the γ bands was just as good as before, and that the effective charge and the quadrupole moments were barely changed. Due to the artificial nature of this calculation, it is pointless to compare its results here with experiment. However, the ease with which a remarkable improvement is obtained might indicate that it is worthwhile to think of making our scheme of calculation slightly less stringent, e.g., by allowing for adding one more term, like a (rather weak) hexadecapole interaction, to our effective interactions, as we have alluded to above.

In Sec. II, we clarified the terminology "micro-

scopic approach." As we emphasized there, to start with realistic single-particle energies is crucial, which we have done. One may still call our work phenomenological because of our use of effective interactions. If the effective interactions are shown to be derivable from more fundamental nucleon-nucleon interactions, however, the theory does not need to be called phenomenological anymore. Note that a good justification of the quadrupole interaction has been given by Kuo and Brown.⁶¹ Further work along this line, in particular the consideration of heavier nuclei, is thus strongly urged.

ACKNOWLEDGMENTS

The authors gratefully thank Dr. H.H. Bolotin, Dr. R.F. Casten, Dr. J.A. Cizewski, and Dr. S. Yates for communications and discussions concerning the experimental data. We also thank Dr. T. Kishimoto and Dr. T. Udagawa for a number of conversations pertaining to the analysis. This work was supported in part by the U.S. Department of Energy.

-
- ¹T. Kishimoto and T. Tamura, Nucl. Phys. A192, 264 (1972).
²T. Kishimoto and T. Tamura, Nucl. Phys. A270, 317 (1976).
³T. Tamura, K. Weeks, and T. Kishimoto, Phys. Rev. C 20, 307 (1979).
⁴K. Weeks and T. Tamura, Phys. Rev. C 22, 888 (1980).
⁵L. Wilets and M. Jean, Phys. Rev. 102, 788 (1956).
⁶R. F. Casten and J. A. Cizewski, Nucl. Phys. A309, 477 (1978).
⁷J. A. Cizewski, R. F. Casten, G. J. Smith, M. R. Macphail, M. L. Stelts, W. R. Kane, H. G. Borner, and W. F. Davidson, Nucl. Phys. A323, 349 (1979).
⁸A. Bohr, K. Dan. Vidensk. Selsk. Mat. Fys. Medd. 26, No. 14 (1952); A. Bohr and B. R. Mottelson, *ibid.* 27, No. 16 (1953).
⁹S. G. Nilsson, K. Dan. Vidensk. Selsk. Mat. Fys. Medd. 29, No. 16 (1955).
¹⁰B. R. Mottelson and S. G. Nilsson, Phys. Rev. 99, 1615 (1955).
¹¹K. J. Weeks and T. Tamura, Phys. Rev. C 21, 2632 (1980).
¹²A. Bohr and B. R. Mottelson, *Nuclear Structure* (Benjamin, New York, 1969), Vol. I, pp. 169, 239, 324, 325, 335, 341.
¹³M. Baranger and K. Kumar, Nucl. Phys. A110, 490 (1968).
¹⁴D. R. Bes and R. A. Broglia, Phys. Rev. C 3, 2349 (1971); 3, 2389 (1971); P. F. Bortignon, R. A. Broglia, D. R. Bes, and R. Liotta, Phys. Rep. 30, 305 (1977).
¹⁵T. Udagawa, T. Tamura, and T. Izumoto, Phys. Lett. 35B, 129 (1971); K. Yagi, K. Sato, Y. Aoki, T. Udagawa, and T. Tamura, Phys. Rev. Lett. 29, 1337 (1972).
¹⁶R. F. Casten, M. R. Macphail, W. R. Kane, D. Breitig, K. Schreckenbach, and J. A. Cizewski, Nucl. Phys. A316, 61 (1979).
¹⁷S. W. Yates, J. C. Cunnane, P. J. Daly, R. Thompson, and R. K. Sheline, Nucl. Phys. A222, 276 (1974).
¹⁸R. Thompson, A. Ikeda, R. K. Sheline, J. C. Cunnane, S. W. Yates, and P. J. Daly, Nucl. Phys. A245, 444 (1975).
¹⁹B. Fogelberg, Nucl. Phys. A197, 497 (1972).
²⁰R. F. Casten, A. I. Namenson, W. F. Davidson, D. D. Warner, and H. G. Borner, Phys. Lett. 76B, 280 (1978).
²¹M. R. Macphail, R. F. Casten, and W. R. Kane, Phys. Lett. 59B, 435 (1975).
²²M. D. Svoren, E. F. Zganjar, and I. L. Hawk, Z. Phys. A 272, 213 (1975).
²³R. F. Casten, H. G. Borner, J. A. Pinston, and W. F. Davidson, Nucl. Phys. A309, 206 (1978).
²⁴R. J. Gehrke, Nucl. Phys. A204, 26 (1973).
²⁵L. K. Wagner, E. B. Shera, G. A. Rinker, and R. K. Sheline, Phys. Rev. C 16, 1549 (1977).
²⁶H. H. Bolotin, I. Katayama, H. Sakai, Y. Fujita, M. Fukiwara, K. Hosono, T. Itahashi, T. Saito, S. H. Sie, D. Conley, D. L. Kennedy, and A. E. Stuchbery (unpublished); H. H. Bolotin, private communications.
²⁷C. Baktash, J. X. Saladin, J. J. O'Brien, and J. G. Alessi, Phys. Rev. C 18, 131 (1978).
²⁸R. M. Ronningen, R. B. Piercey, A. V. Ramayya, J. H. Hamilton, S. Raman, P. H. Stelson, and W. K. Dagenhart, Phys. Rev. C 16, 571 (1977).
²⁹N. R. Johnson, P. P. Hubert, E. Eichler, D. G.

- Sarantites, J. Urbon, S. W. Yates, and T. Lindblad, *Phys. Rev. C* **15**, 1325 (1977).
- ³⁰J. F. W. Jansen, and H. Pauw, *Nucl. Phys.* **A94**, 235 (1967).
- ³¹M. Finger, R. Foucher, J. P. Husson, J. Jastrzebski, A. Johnson, G. Astner, B. R. Erdal, A. Kjelberg, P. Patzelt, A. Hogland, S. G. Malmskog, and R. Henck, *Nucl. Phys.* **A188**, 369 (1972).
- ³²S. A. Hjorth, A. Johnson, T. Lindblad, L. Funke, P. Kemnitz, and G. Winther, *Nucl. Phys.* **A262**, 328 (1976).
- ³³B. Singh and M. W. Johns, *Nucl. Phys.* **A208**, 55 (1973).
- ³⁴W. E. Cleveland and E. Zganjar, *Z. Phys. A* **279**, 195 (1976).
- ³⁵S. W. Yates, private communication.
- ³⁶A. Arima and F. Iachello, *Phys. Rev. Lett.* **40**, 385 (1978), and references therein.
- ³⁷R. F. Casten, J. S. Greenberg, S. H. Sie, G. A. Burginyon, and D. A. Bromley, *Phys. Rev.* **187**, 1532 (1969).
- ³⁸M. Hoehn, E. B. Shera, Y. Yamazaki, and R. M. Steffen, *Phys. Rev. Lett.* **39**, 1313 (1977).
- ³⁹J. E. Glenn, R. J. Pryor, and J. X. Saladin, *Phys. Rev.* **188**, 1905 (1969).
- ⁴⁰G. D. Benson, A. V. Ramayya, R. G. Albridge, and G. D. O'Kelley, *Nucl. Phys.* **A150**, 311 (1970).
- ⁴¹H. Helppi, A. Pakkanen, and J. Hattula, *Nucl. Phys.* **A223**, 13 (1974).
- ⁴²W. T. Milner, F. K. McGowan, R. L. Robinson, P. H. Stelson, and R. O. Sayer, *Nucl. Phys.* **A177**, 1 (1971).
- ⁴³I. Berkes, R. Rougny, M. Meyer-Levy, R. Chery, J. Daniere, G. Lhersonneau, and A. Troncy, *Phys. Rev. C* **6**, 1098 (1973).
- ⁴⁴W. C. King, Z. W. Grabowski, and R. P. Scharenberg, *Phys. Rev. C* **4**, 1382 (1971).
- ⁴⁵F. Wagner, D. Kucheida, G. Kaindl, and P. Kienle, *Z. Phys.* **230**, 80 (1970).
- ⁴⁶P. Sioshansi, D. A. Garber, Z. W. Grabowski, R. P. Scharenberg, R. M. Steffen, and R. M. Wheeler, *Phys. Rev. C* **6**, 2245 (1972).
- ⁴⁷H. A. Doubt, J. B. Fechner, K. Hagemeyer, and K. H. Speidel, *Z. Phys.* **254**, 339 (1972).
- ⁴⁸D. A. Garber, M. Behar, Z. W. Grabowski, and W. C. King, *Z. Phys.* **270**, 163 (1974).
- ⁴⁹F. T. Baker, *Nucl. Phys.* **A331**, 39 (1979), and references therein.
- ⁵⁰K. Kumar, *Phys. Lett.* **29B**, 25 (1969).
- ⁵¹V. I. Isador and I. Kh. Lemberg, *Pis'ma Zh. Eksp. Teor. Fiz.* **9**, 698 (1969) [*JETP Lett.* **9**, 438 (1969)].
- ⁵²F. J. W. Hahne, T. Tamura, and K. J. Weeks (unpublished).
- ⁵³R. J. Turner and T. Kishimoto, *Nucl. Phys.* **A217**, 317 (1973).
- ⁵⁴K. Kumar and M. Baranger, *Nucl. Phys.* **A122**, 273 (1968).
- ⁵⁵U. Gotz, H. C. Pauli, K. Alder, and K. Junker, *Nucl. Phys.* **A192**, 1 (1972).
- ⁵⁶V. Strutinski, *Nucl. Phys.* **A95**, 420 (1967).
- ⁵⁷O. Scholten, *Interacting Bosons in Nuclear Physics*, edited by F. Iachello (Plenum, New York, 1979), p. 17.
- ⁵⁸T. Otsuka, A. Arima, F. Iachello, and I. Talmi, *Phys. Lett.* **76B**, 139 (1978).
- ⁵⁹H. H. Hsu, F. K. Wahn, and S. A. Williams, *Phys. Rev. C* **19**, 1550 (1979).
- ⁶⁰H. L. Yadav, H. Toki, and A. Faessler, *Phys. Lett.* **76B**, 144 (1978); B. Castel, A. Faessler, H. Toki, and H. L. Yadav, *Jülich, Annual Report* (1978).
- ⁶¹T. T. S. Kuo and G. E. Brown, *Nucl. Phys.* **85**, 40 (1966).